FILAMENTARY STRUCTURE IN THE ORION MOLECULAR CLOUD

JOHN BALLY
AT & T Bell Laboratories

WILLIAM D. LANGER
Princeton University

AND

ANTONY A. STARK AND ROBERT W. WILSON
AT & T Bell Laboratories

ABSTRACT

We present a large-scale ^{13}CO map (containing 33,000 spectra on a 1' grid) of the giant molecular cloud located in the southern part of Orion which contains the Orion Nebula, NGC 1977, and the L1641 dark cloud complex. The overall structure of the cloud is filamentary, with individual features having a length up to 40 times their width. The northern portion of the cloud is compressed, dynamically relaxed, and supports massive star formation. In contrast, the southern part of the Orion A cloud is diffuse, exhibits chaotic spatial and velocity structure, and supports only intermediate- to low-mass star formation. This morphology may be the consequence of the formation and evolution of the Ori OB I association centered north of the molecular cloud. The entire cloud, in addition to the 5×10^3 $M_\odot$ filament containing both OMC-1 and OMC-2, exhibits a north-south velocity gradient. Implications of the observed cloud morphology for theories of molecular cloud evolution are discussed.

Subject headings: interstellar: molecules — nebulae: Orion Nebula

I. INTRODUCTION

We present a detailed ^{13}CO survey of the Orion A molecular cloud in order to investigate the internal structure and kinematics of a massive star-forming molecular cloud. The Orion region contains the nearest giant molecular clouds (GMCs) to the Sun. Extensive low-resolution (8') mapping of the ^{12}CO emission in this region (Kutner et al. 1977; Chin 1978; Maddalena et al. 1986) demonstrated the existence of two giant clouds, one located in the northern part of Orion, and one in the southern part, behind the Orion Nebula, each having a mass around 10^5 $M_\odot$. Located at a distance of 500 pc, the clouds are situated 10° to 14° below the Galactic plane toward the outer Galaxy, well away from potentially confusing background clouds. The more abundant ^{12}CO species is optically thick along most lines of sight and is suited as a probe of the kinetic temperature near the front surface of the cloud where the optical depth is unity. The rarer ^{13}CO species is optically thin in most directions, as demonstrated by $C^{18}O$ observations, and therefore its brightness is a probe of the column density of molecular gas through the entire cloud.

II. OBSERVATIONS

All data presented here were obtained during the winter 1984–1985 and 1985–1986 observing seasons with the AT & T Bell Laboratories 7 m diameter offset Cassegrain millimeter-wavelength antenna located at Crawford Hill in Holmdel, N.J. An SIS receiver with a single-sideband receiver tempera-

ture ranging from 90 to 200 K was used in conjunction with both a 128 channel 0.25 MHz filterbank and a spectrum expander (Henry 1976) giving 128 channels at 100 kHz resolution. Most data were obtained in the frequency-switched mode using frequency offsets of 3.2 and −3.2 MHz, which places both the signal and reference frequencies within the passband of the 100 kHz filterbank. Integration times were chosen automatically to yield a channel-to-channel rms noise of 0.3 K in the folded 100 kHz filters.

After folding of the spectra, first-order baselines were fitted to those channels not containing a signal and were then subtracted from the data. Spectra were interpolated onto a standard 30" grid and then displayed with the NRAO-AIPS software package. Gray-scale images were produced with a Dicomed at the National Radio Astronomy Observatory.

We estimate the mass of features in the map from the formula

$$M(\mathrm{H_2}) = \mu m_{\mathrm{H_2}} \int_S N(\mathrm{H_2}) \, dS,$$

where

$$N(\mathrm{H_2}) \approx \frac{1.49 \times 10^{20} \left[\mathrm{cm^{-2} (K \ km \ s^{-1})^{-1}} \right] \int T_A^*(^{13}\mathrm{CO}) \, dV}{\eta [1 - e^{-(5.29 \ \mathrm{K}/T_{ex})}]},$$

assuming a ratio $N(\mathrm{H_2})/N(^{13}\mathrm{CO}) = 7 \times 10^5$ (Frerking, Langer, and Wilson 1982), where S is the projected surface
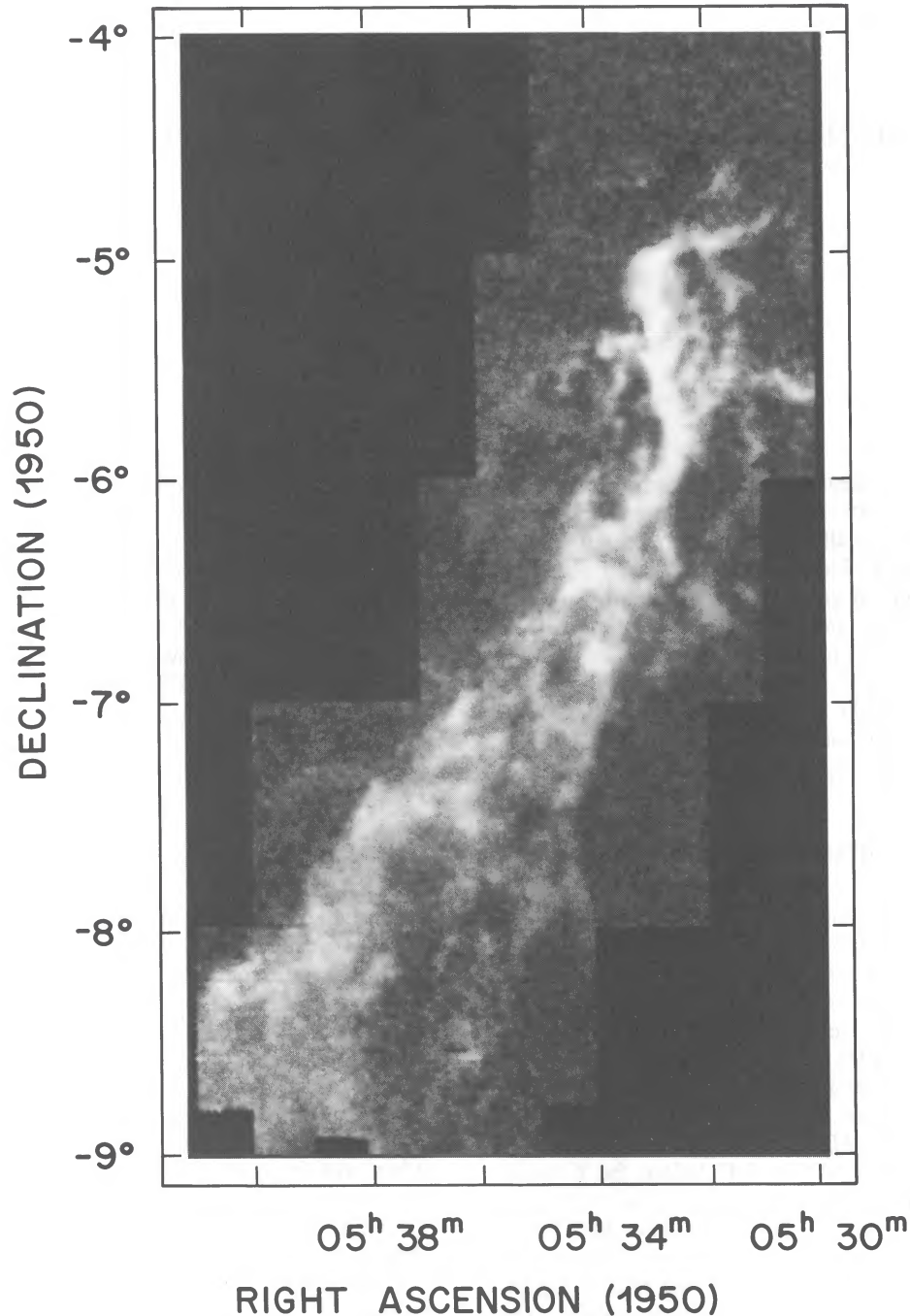
FIG. 1.—A gray-scale representation of the integrated ^{13}CO emissivity $\int T_A^*(V)\,dV$ in the southern portion of Orion. The intensity represented ranges from 0 to 54 K km s^{-1}.

area of the region whose mass is being evaluated, η is the antenna primary beam efficiency, and μ (≈ 1.3) is the mean molecular weight per particle.

III. STRUCTURE OF THE ORION A MOLECULAR CLOUD

Figure 1 shows a gray-scale intensity map of the ^{13}CO emission in the Orion A GMC integrated from $V_{LSR} = 2.5$ km s^{-1} to $V_{LSR} = 13.5$ km s^{-1}. The total amount of molecu-

lar gas seen in this map (which covers 8 deg^2) is 5×10^4 $M_\odot$, about one-half the amount estimated to be associated with the 29 deg^2 region around the Orion A cloud by Maddalena *et al.* (1986) from ^{12}CO observations. The most intense feature in the ^{13}CO map is the 1°.5 elongated $\int$-shaped filament located in the northern part of the cloud. This feature contains NGC 1977 at its northern end, the Orion Nebula in the middle, and its southern end trails off about 20′ north of NGC 1999. This filament is about 0.5 pc wide, at least 13 pc long, and has a

mass of 5×10^3 $M_\odot$, 25% of the total mass of the mapped region.

Individual 1 km s^{-1} wide channel maps (Figs. 2 and 3 [Pls. L3 and L4] demonstrate that all of the major structures seen in ^{13}CO in the Orion A cloud are composed of many smaller clumps and filaments. In addition to the dominant northern filament containing M42, there are three or four large filaments and many small ones. About 30% of the emission below $\delta = -6°$ is contained in a clumpy ridge oriented parallel to the Galactic plane. This structure is on average about 20' wide and more than 3° long. At velocities between $V_{LSR} = 6$–8 km s^{-1}, a second filament running nearly north-south intersects this ridge near an intense bright spot centered at $\alpha = 6^h36^m$ and $\delta = -6°25'$. The overall shape of the ridge and this second filament is cometary and points toward both the M42 H II region and the center of the Ori OB I association. This morphology is similar to the cometary globules seen in the Gum nebula (Reipurth 1984).

Well over 100 individual condensations can be identified in the Orion A cloud. From excitation arguments, the ^{13}CO emitting gas must have a density of $\bar{n} > 500$ cm^{-3}. The properties of some typical well-defined clumps in 10 distinct regions of the Orion A cloud are given in Table 1 and illustrated in Figure 4. The clump boundaries were defined at 50% of the local peak surface brightness. Of these 10 fields, two had two distinct lumps along the line of sight, and one had three. The large linewidth of clump 5b suggests that it may consist of two blended, unresolved components. The internal velocity dispersion of individual clumps, as measured by the Gaussian fit to the line profiles near the clump centers, scale roughly as $\Delta V_{FWHM} = 0.54$ km s$^{-1}(M/M_\odot)^{0.25}$. Individual clumps have properties similar to those seen in the Rosette molecular cloud (Blitz and Stark 1986) and the cores seen in the filamentary Taurus molecular clouds (Myers and Benson 1983), except that in Orion these structures are more densely packed.

There is an interclump gas which produces weak ^{13}CO emission. This component produces 25% of the flux from the GMC, implying that the fraction of mass in the interclump gas, θ_{in}, is 25%, and the fraction of mass in the filaments θ_{fil} is 75% as judged by the ^{13}CO column densities. If the volume filling factor, $f_{fil} = 10\%$ for the filamentary gas, corresponding to a projected area filling factor of 30% (which implies that the interclump gas has a volume filling factor $f_{in} = 90\%$), then the mean interclump density is $n_{in} = \bar{n}f_{fil}\theta_{in}/f_{in}\theta_{fil} > 40$ cm^{-3}. The interclump gas probably consists of small, beam-diluted structures and subthermally excited gas, and atomic gas which is invisible to our observations.

The clumping factor

$$C = \frac{A \int_A \sigma^2 \, dA}{\left(\int \sigma \, dA \right)^2}$$

defined by Hut and Tremaine (1985) (where σ is the cloud surface density and the integral is over the mapped surface area of the cloud) is a useful quantitative measure of the

degree of lumpiness in the molecular cloud. For the mapped field, we find $C = 2.7$, much greater than that of a homogeneous spherical cloud which has $C = 9/8$.

The observed clumpy and filamentary cloud morphology affects the longevity of the entire molecular cloud. The observed surface filling factor of the clumps and filaments appears to be about 30%. From the overall dispersion of the velocity centroids, we estimate that the clumps and filaments have random rms velocities of about 2 km s^{-1} relative to the mean cloud velocity. The crossing time of these lumps is 5×10^6 yr. With a 30% projected surface filling factor and ignoring the drag effects of the interclump medium, each core can be expected to survive for 1.5×10^7 yr before encountering another core. The core-core collision time is therefore many times the free-fall time of the whole GMC.

There is an overall velocity gradient shown in Figures 2 and 3, ranging from $V_{LSR} = 4$ km s^{-1} in the south to $V_{LSR} = 12$ km s^{-1} in the north. In Figure 5, the velocity field along the northern filament abruptly changes at the Orion Nebula from $V_{LSR} = 11$ km s^{-1} to the north to $V_{LSR} = 7$ km s^{-1} in the south. The dominant concentration of mass in this region lies directly behind the Orion Nebula as indicated by the ^{13}CO column density and $J = 2$–1 CS observations (to be presented in a later paper). A comparison between the gravitational and centrifugal forces indicates rotation about an east-west axis. For a rotation velocity of 1.75 km s^{-1} 4.5 pc from the center (implying a rotation period of 16 Myr), the computed dynamic mass is $M_{dyn} = R(\Delta V)^2/G \approx 3 \times 10^3$ $M_\odot$, only slightly smaller than the total mass derived from ^{13}CO column densities.

Although the observed velocity structure can be explained as rotation about the mass centered behind the Nebula, we believe that this structure is a filament rather than an edge-on dish for several reasons.

1. Although the H II region M42 is located within 1 pc or so of the molecular cloud core, there is little foreground extinction, indicating that there is not as much mass on the near side of the molecular ridge as would be expected for an edge-on disk if the nebula were located near its center.

2. If the ^{13}CO structure were an edge-on disk, its plane of symmetry would have to lie within a few degrees of our line of sight to preserve its large aspect ratio, an unlikely situation.

3. Although the ends of this structure are curved, the projected thickness of the gas layer remains small; for a warped disk, the apparent thickness of the layer would be larger where warping is stronger.

4. If the ridge were a 9 pc diameter, 0.5 pc thick disk, the mean volume density would be about 300 cm^{-3}. Most of the ridge is bright in the $J = 2$–1 CS line which requires a density in excess of 5×10^3 cm^{-3} for collisional excitation. For a 5×10^3 $M_\odot$ cylinder, 0.5 pc in diameter and 9 pc long, the mean H$_2$ density is about 4×10^4 cm^{-3}, consistent with the detection of CS.

Four global properties of the Orion A cloud provide clues to its past evolutionary history.

1. There is a large overall velocity gradient along the entire length of the cloud with the same sense as the rotation of the major filament.

2. Summing the emission across the cloud in constant declination strips shows that the mass in each strip is the

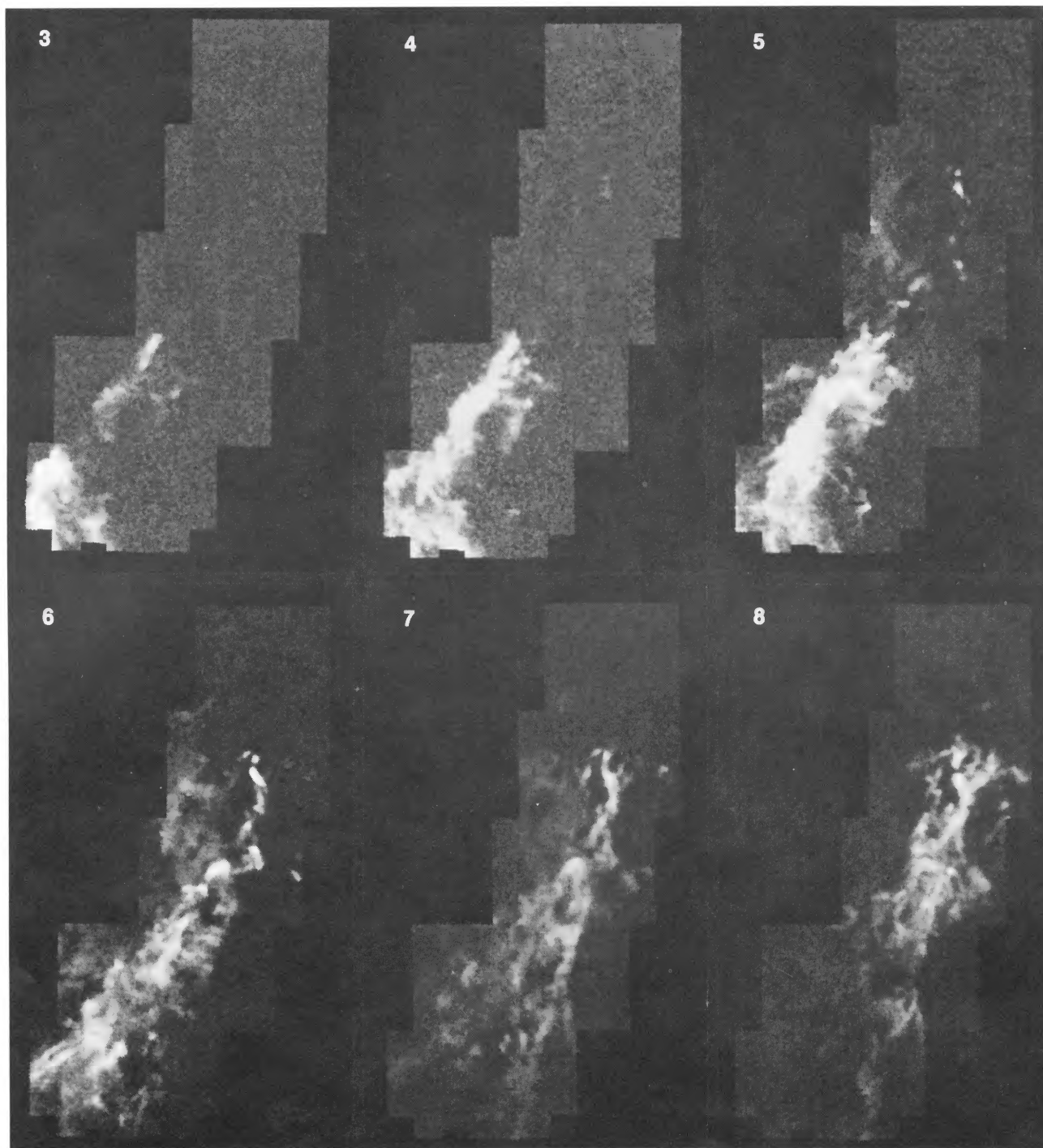FIG. 2.—A montage of six gray-scale images showing the emission in 1 km s^{-1} wide velocity steps. The maps cover central velocities from $V_{LSR} = $ 3–8 km s^{-1}. The intensities displayed range from -1 K km s^{-1} to an upper value of 9, 6, 7, 9, 15, and 15, respectively, for each of the six images beginning with the frame showing the 3 km s^{-1} map.

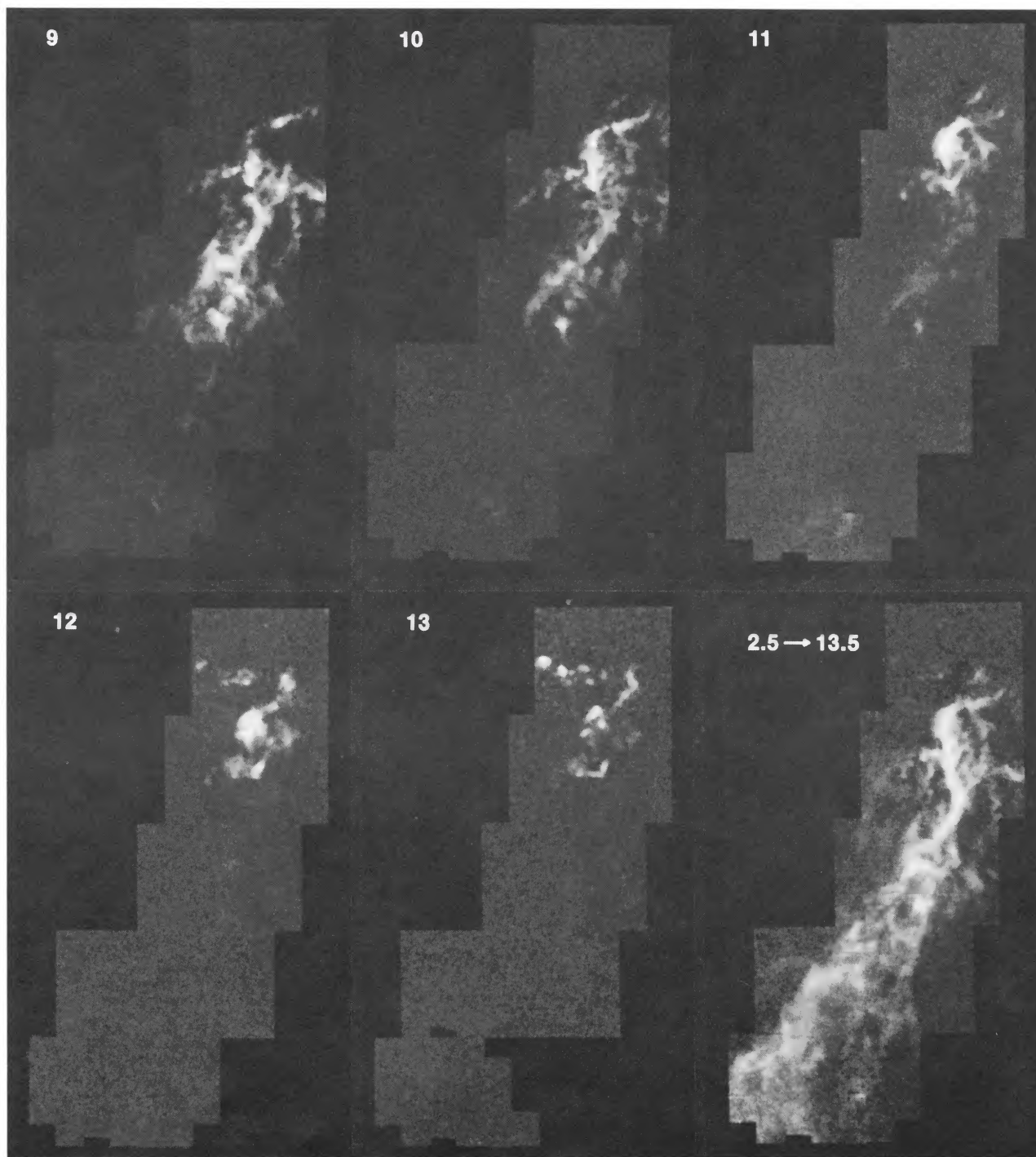BALLY, LANGER, STARK, AND WILSON (see page L47)

FIG. 3.—Continuation of Fig. 2 showing the velocities from 9 to 13 km s^{-1}. The final plate in the lower right shows the integrated emission from V_{LSR} = 2.5–13.5 km s^{-1}. The intensities displayed range from -1 K km s^{-1} to an upper value of 15, 14, 14, 12, 8, and 55, respectively, for each of the six images beginning with the same frame showing the 9 km s^{-1} map.

BALLY, LANGER, STARK, AND WILSON (see page L47)

TABLE 1

TYPICAL ORION A CLUMP PROPERTIES

| Clump Number	α(1950)	δ(1950)	V_{LSR} (km s^{-1})	ΔV (km s^{-1})	Area (arcmin^2)	Mass ($M_\odot$)	$T(^{12}CO)$ (K)	$T(^{13}CO)$ (K)	$\int T\,dV$ (K km s^{-1})	Comments
1	05^{h}32^{m}47^s	−5°24′30″	8.6	3.7	108	2200	76	14.9	57.3	BNKL–Orion A
2	05 32 36	−5 43 20	7.9	2.8	63	900	23.4	9.3	27.1	South of BNKL
3	05 33 52	−6 47 20	8.7	2.9	72	460	21.8	10.6	30.7	NGC 1999
4	05 33 55	−6 24 00	7.5	2.7	133	730	19.4	12.1	31.9	20′N of NGC 1999
5a	05 32 40	−6 17 20	6.1	1.9	54	66	10.8	6.4	11.0	HH 33 and HH 40
5b	05 32 40	−6 17 20	9.0	3.8	54	74	12.0	4.1	12.5	HH 33 and HH 40
6	05 33 01	−6 28 40	8.4	1.3	20	110	26.6	11.0	16.9	HH 34 region
7	05 34 43	−4 30 00	13.0	1.2	33	38	20.0	8.2	10.9	Knot N of NGC 1977
8	05 40 25	−8 16 00	3.0	1.7	72	117	12.6	8.4	13.8	Near S edge of map
9	05 38 52	−8 08 00	5.1	2.2	72	194	12.8	2.7	16.7	In southern filament
10a	05 37 51	−7 31 00	4.1	2.4	102	144	11.2	5.9	10.4	Near object 50
10b	05 38 03	−7 26 00	6.4	1.6	102	77	10	4.9	9.4	Near object 50
11a	05 36 22	−7 03 00	3.7	1.7	84	49	10.8	6.8	14.5	Three components
11b	05 36 14	−7 06 00	5.9	2.0	84	58	9.7	5.2	12.6	Three components
11c	05 36 02	−6 57 00	6.7	1.0	84	17	14.2	6.6	6.6	Three components
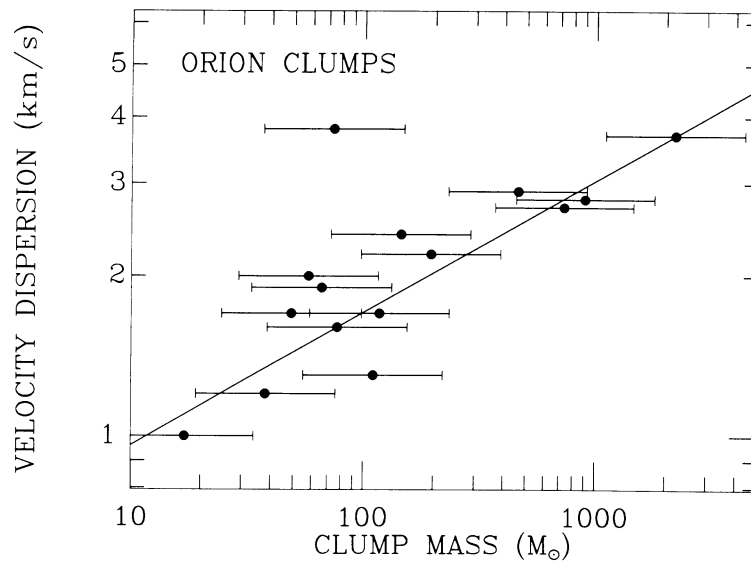
FIG. 4.—A plot of clump mass vs. internal velocity dispersion derived for 15 easily identified clumps derived from 10 separate fields in the maps shown in Figs. 1 and 2. The error bars represent a factor of 2 uncertainty in the mass estimate. The line represents the function $\Delta V_{FWHM} = 0.5\ M^{0.25}$, a reasonable representation of the data given in Table 1.

same. That is, the dense and narrow major filament in the north has about the same mass per unit length as does the more diffuse southern portion of the cloud. This similarity implies that the northern part of the cloud has been compressed.

3. In the southern part of the molecular cloud, broad and multiple velocity component line profiles are common, indicating that along many lines of sight, several individual features exist at velocities differing by a few km s^{-1}. In contrast, north of $\delta = -6°$, mostly single-velocity components are seen, implying that the more compressed northern portion of the cloud is also dynamically more relaxed.

4. Massive star formation of the gas several degrees to the south shows signs of being influenced by this activity. Some of the cloud cores, including the ones associated with cometary filaments, have optically bright rims on their northern sides.

We suggest that the properties of the Orion A cloud can be explained as resulting from the compression of the interstellar medium by a superbubble driven by the Orion OB association. The formation of the first OB stars 1 to 2 × 10^7 yr ago (Blaauw 1964) initiated the expansion of a hot bubble which drives a shock capable of snowplowing mass from the surrounding medium. Today, the outer edge of this bubble extends 30° across the sky from the eastern edge of Orion to the constellation of Cetus (Cowie, Songaila, and York 1979). The bubble is driven by the combined energy input of H II regions, stellar winds, and supernova explosions produced by about a hundred O and B stars. Refraction of the shock by a preexisting small cloud of dense gas (McKee and Cowie 1975; Rozyczka and Tenorio-Tagle 1985) will produce a conical wake (bow shock) in the flow. If the shock is in the snowplow (isothermal) stage and the sound speed in the interior of the bubble exceeds the velocity of the refracted shock, then the
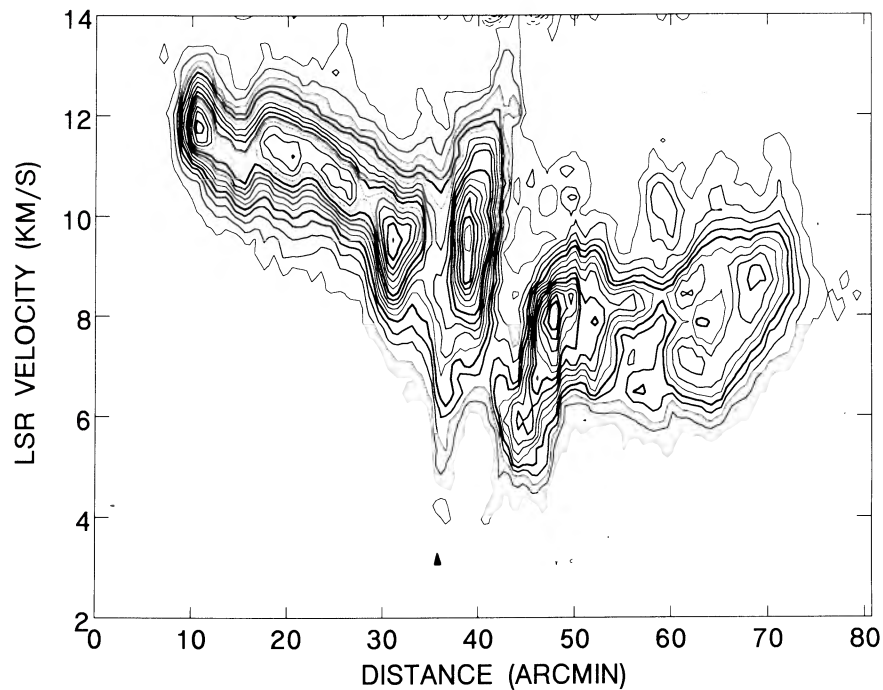
FIG. 5.—A ^{13}CO spatial-velocity cut along the molecular filament containing the Orion molecular cloud, starting at $\alpha(1950) = 5^h33^m08^s.2$, $\delta(1950)$ = $-4°50'00''$ and ending at $\alpha(1950) = 5^h32^s24^s.2$, $\delta(1950) = -6°10'00''$. Contour levels are at intervals of 1 K. The filled triangle marks the position of IRc2, the core of the BNKL region, located just north of M32.

high-pressure bubble will compress the original cloud and deposit mass from the swept-up postshock layer in the wake behind the cloud. The interior of the Orion superbubble contains gas having velocities over 100 km s^{-1} with a similar sound speed (Cowie, Songaila, and York 1979) and the outer shock containing the cold swept-up gas has a measured expansion velocity of 5–20 km s^{-1}. Therefore, the opening angle of the bow shock decreases with time leading to a conical structure with a highly compressed apex similar to the morphology seen in our maps of Orion. If the Orion A cloud was shaped by this mechanism, the outer boundary of the

superbubble should lie to the southeast of the molecular cloud. Barnard's Loop, the edge of the Orion superbubble, lies just beyond the southern edge of our ^{13}CO map. Further support for this model is provided by the observation that the northern portion of the cloud, which is more deeply embedded in the superbubble, has experienced more compression. This region is more dynamically relaxed than the southern part of the cloud and is the site of massive star formation (points 2–4 above). This model explains part of the observed velocity gradient as a remnant of the velocity field of the layer deposited behind the preexisting cloud (point 1 above).

REFERENCES

Blaaw, A. 1964, *Ann. Rev. Astr. Ap.*, **2**, 213.
Blitz, L., and Stark A. A. 1986, *Ap. J. (Letters)*, **300**, L89.
Chin, G. 1978, Ph.D. thesis, Columbia University.
Cowie, L. L., Songaila, A., and York, D. G. 1979, *Ap. J.*, **230**, 469.
Frerking, M. A., Langer, W. D., and Wilson, R. W. 1982, *Ap. J.*, **262**, 590.
Henry, P. S. 1976, *Rev. Sci. Instr.*, **47**, 1020.
Hut, P., and Tremaine, S. 1985, *A.J.*, **90**, 1548.
Kutner, M. L., Tucker, K. D., Chin, G., and Thaddeus, P. 1977, *Ap. J.*, **215**, 521.

Maddalena, R. 1986, Ph.D. thesis, Columbia University.
Maddalena, R. J., Morris, M., Moscowitz, J., and Thaddeus, P. 1986, *Ap. J.*, **303**, 375.
McKee, C. F., and Cowie, L. L. 1975, *Ap. J.*, **195**, 715.
Myers, P., and Benson, P. 1983, *Ap. J.*, **266**, 309.
Reipurth, B. 1983, *Astr. Ap.*, **117**, 183.
Rozyczka, M., and Tenorio-Tagle, G. 1985, *Astr. Ap.*, **147**, 220.

JOHN BALLY, ANTONY A. STARK, and ROBERT W. WILSON: AT & T Bell Laboratories, Crawford Hill, Box 400, Holmdel, NJ 07733

WILLIAM D. LANGER: Plasma Physics Laboratory, Princeton University, P.O. Box 451, Princeton, NJ 08544